Langevin thermostat for rigid body dynamics

Ruslan L. Davidchack,[a] Richard Handel, and M. V. Tretyakov
Department of Mathematics, University of Leicester, Leicester LE1 7RH, United Kingdom

(Received 27 January 2009; accepted 15 May 2009; published online 15 June 2009)

We present a new method for isothermal rigid body simulations using the quaternion representation and Langevin dynamics. It can be combined with the traditional Langevin or gradient (Brownian) dynamics for the translational degrees of freedom to correctly sample the canonical distribution in a simulation of rigid molecules. We propose simple, quasisymplectic second-order numerical integrators and test their performance on the TIP4P model of water. We also investigate the optimal choice of thermostat parameters. © *2009 American Institute of Physics*. [DOI: 10.1063/1.3149788]

I. INTRODUCTION

Classical molecular dynamics simulation of an isolated system naturally samples states from a microcanonical (*NVE*) ensemble, where the number of particles N, volume V, and total energy of the system E are held constant. However, in many cases it is desirable to study the system in a more experimentally relevant canonical (*NVT*) ensemble, where the temperature T is specified instead of E. In order to sample from the canonical ensemble, the molecular dynamics equations of motion are modified by introducing the interaction of the system with a "thermostat." There exist a large variety of approaches for introducing such a thermostat, which can be roughly classified into two categories: deterministic and stochastic, depending on whether the resulting equations of motion contain a random component (for a review, see, e.g., Ref. 1).

Among various deterministic approaches, those based on coupling the system to a few external degrees of freedom (e.g., Nosé–Hoover thermostat) have become very popular. Given ergodicity in the molecular system dynamics, such thermostats are proven to generate correct canonical ensemble sampling of the system phase space. However, since the thermostat variables are coupled and control directly only global system quantities (e.g., kinetic energy), such thermostats rely on the efficient energy transfer within the system to achieve *equipartition* within the canonical distribution, such that the average energy of each degree of freedom within the system is equal to k_BT. Therefore, in a system where the energy transfer between its different parts is slow (e.g., systems combining fast and slow degrees of freedom), the simple Nosé–Hoover thermostat may have difficulty maintaining the same temperature for the different parts of the system. In this case more complicated thermostats are necessary, for example, Nosé–Hoover chain thermostat, or separate thermostats for different parts of the systems (see, e.g., Ref. 2).

The stochastic approach exploits ergodic stochastic differential equations (SDEs) with the Gibbsian (canonical ensemble) invariant measure. For this purpose, Langevin-type equations or gradient systems with noise can be used (see, e.g., Refs. 3–7 and references therein). Stochastic thermostats, with their independent thermalization of each degree of freedom, provide direct control of equipartition and thus do not need to rely on the efficient energy transfer within the system.

In order to achieve such a direct thermalization of the system, one needs to be able to apply stochastic thermostats to all types of degrees of freedom. The standard Langevin equations for translational degrees of freedom are well known, while Langevin thermostats for systems with constraints have been proposed quite recently.[8,9] In this paper we introduce Langevin equations for the rigid body dynamics in the *quaternion representation* and propose effective second-order quasisymplectic numerical integrators for their simulation. These equations can be coupled either with Langevin or Brownian dynamics for the translational degrees of freedom.

In Sec. II we recall the Hamiltonian system for rigid body dynamics in the quaternion representation from Ref. 10, based on which we derive Langevin and gradient-Langevin thermostats. Second-order (in the weak sense) numerical methods for these stochastic systems are constructed in Sec. III. We test the thermostats and the proposed numerical integrators on the TIP4P model of water.[11] The results of our numerical experiments are presented in Sec. IV. In particular, we investigate the optimal choice of thermostat parameters and the discretization error of the numerical methods. A summary of the obtained results is given in Sec. V.

II. EQUATIONS OF MOTION

We consider a system of n rigid three-dimensional molecules described by the center-of-mass coordinates $\mathbf{r}=(r^{1\mathsf{T}},\ldots,r^{n\mathsf{T}})^{\mathsf{T}}\in\mathbb{R}^{3n}$, $r^j=(r_1^j,r_2^j,r_3^j)^{\mathsf{T}}\in\mathbb{R}^3$, and the rotational coordinates in the quaternion representation $\mathbf{q}=(q^{1\mathsf{T}},\ldots,q^{n\mathsf{T}})^{\mathsf{T}}\in\mathbb{R}^{4n}$, $q^j=(q_0^j,q_1^j,q_2^j,q_3^j)^{\mathsf{T}}\in\mathbb{R}^4$, such that $|q^j|=1$ (for further background on the quaternion representation of rigid body dynamics, see e.g., Refs. 12–14). We use standard matrix notations, and "T" denotes transpose. Following Ref. 10, we write the system Hamiltonian in the form

[a]Electronic mail: rld8@mcs.le.ac.uk.

$$H(\mathbf{r},\mathbf{p},\mathbf{q},\boldsymbol{\pi}) = \frac{\mathbf{p}^{\mathsf{T}}\mathbf{p}}{2m} + \sum_{j=1}^{n}\sum_{l=1}^{3} V_l(q^j,\pi^j) + U(\mathbf{r},\mathbf{q}), \tag{1}$$

where $\mathbf{p}=(p^{1\mathsf{T}},\ldots,p^{n\mathsf{T}})^{\mathsf{T}} \in \mathbb{R}^{3n}$, $p^j=(p_1^j,p_2^j,p_3^j)^{\mathsf{T}} \in \mathbb{R}^3$, are the center-of-mass momenta conjugate to $\mathbf{r}$, $\boldsymbol{\pi}=(\pi^{1\mathsf{T}},\ldots,\pi^{n\mathsf{T}})^{\mathsf{T}} \in \mathbb{R}^{4n}$, $\pi^j=(\pi_0^j,\pi_1^j,\pi_2^j,\pi_3^j)^{\mathsf{T}} \in \mathbb{R}^4$, are the angular momenta conjugate to $\mathbf{q}$, and $U(\mathbf{r},\mathbf{q})$ is the potential interaction energy. The second term represents the rotational kinetic energy of the system with

$$V_l(q,\pi) = \frac{1}{8I_l}[\pi^{\mathsf{T}} S_l q]^2, \quad q,\pi \in \mathbb{R}^4, \quad l=1,2,3, \tag{2}$$

where the three constant four-by-four matrices S_l are such that

$$S_1 q = (-q_1,q_0,q_3,-q_2)^{\mathsf{T}}, \quad S_2 q = (-q_2,-q_3,q_0,q_1)^{\mathsf{T}},$$

$$S_3 q = (-q_3,q_2,-q_1,q_0)^{\mathsf{T}},$$

and I_l are the principal moments of inertia of the rigid molecule. The Hamilton equations of motion are

$$\frac{d\mathbf{r}}{dt} = \frac{\mathbf{p}}{m}, \quad \frac{d\mathbf{p}}{dt} = -\nabla_{\mathbf{r}} U(\mathbf{r},\mathbf{q}),$$

$$\frac{dq^j}{dt} = \sum_{l=1}^{3} \nabla_{\pi^j} V_l(q^j,\pi^j),$$

$$\frac{d\pi^j}{dt} = -\sum_{l=1}^{3} \nabla_{q^j} V_l(q^j,\pi^j) - \nabla_{q^j} U(\mathbf{r},\mathbf{q}),$$

$$j=1,\ldots,n. \tag{3}$$

It is easy to check that if the initial conditions are chosen such that $|q^j(0)|=1$, then the corresponding Hamilton equations of motion ensure that

$$|q^j(t)| = 1, \quad j=1,\ldots,n \ \text{ for all } \ t \geq 0. \tag{4}$$

In the rest of this section we derive stochastic thermostats for this molecular system, which preserve Eq. (4). They take the form of ergodic SDEs with the Gibbsian (canonical ensemble) invariant measure possessing the density

$$\rho(\mathbf{r},\mathbf{p},\mathbf{q},\boldsymbol{\pi}) \propto \exp(-\beta H(\mathbf{r},\mathbf{p},\mathbf{q},\boldsymbol{\pi})), \tag{5}$$

where $\beta=1/(k_B T)>0$ is an inverse temperature.

A. Langevin-type equations

Consider the Langevin-type equations (in the form of Ito),[15]

$$dR^j = \frac{P^j}{m}dt, \quad R^j(0)=r^j,$$

$$dP^j = -\nabla_{r^j} U(\mathbf{R},\mathbf{Q})dt - \gamma g(P^j,R^j)dt + b(R^j)dw^j(t), \quad P^j(0)=p^j,$$

$$dQ^j = \sum_{l=1}^{3} \nabla_{\pi^j} V_l(Q^j,\Pi^j)dt, \quad Q^j(0)=q^j, \quad |q^j|=1,$$

$$d\Pi^j = -\sum_{l=1}^{3} \nabla_{q^j} V_l(Q^j,\Pi^j)dt - \nabla_{q^j} U(\mathbf{R},\mathbf{Q})dt - \Gamma G(Q^j,\Pi^j)dt + B(Q^j,\Pi^j)dW^j(t), \quad \Pi^j(0)=\pi^j,$$

$$j=1,\ldots,n, \tag{6-7}$$

where $\gamma \geq 0$ and $\Gamma \geq 0$ with $\gamma\Gamma>0$ are the friction coefficients for the translational and rotational motions, respectively, measured in units of inverse time, which control the strength of coupling of the system to the "heat bath;" g is a three-dimensional appropriately normalized vector; G is a four-dimensional vector, which provides a balance in coupling various rotational degrees of freedom with the heat bath; b and B are three-by-three and four-by-four matrices, respectively; and $(\mathbf{w}^{\mathsf{T}},\mathbf{W}^{\mathsf{T}})^{\mathsf{T}}=(w^{1\mathsf{T}},\ldots,w^{n\mathsf{T}},W^{1\mathsf{T}},\ldots,W^{n\mathsf{T}})^{\mathsf{T}}$ is a $(3n+4n)$-dimensional standard Wiener process with $w^j=(w_1^j,w_2^j,w_3^j)^{\mathsf{T}}$ and $W^j=(W_0^j,W_1^j,W_2^j,W_3^j)^{\mathsf{T}}$.

For simplicity, we assumed here that g, G, b, and B are the same for all n molecules, although one could choose them depending on the molecule number j. The latter can be especially useful for systems consisting of significantly different types of molecules. It is also natural to require that each degree of freedom is thermalized by its own independent noise, and in what follows we assume that the matrices b and B are diagonal. Further, we suppose that the coefficients of system (6)-(7) are sufficiently smooth functions and the process $X(t)=(\mathbf{R}^{\mathsf{T}}(t),\mathbf{P}^{\mathsf{T}}(t),\mathbf{Q}^{\mathsf{T}}(t),\boldsymbol{\Pi}^{\mathsf{T}}(t))^{\mathsf{T}}$ is ergodic, i.e., there exists a unique invariant measure μ of X and independently of $x \in \mathbb{R}^{14n}$ there exists the limit

$$\lim_{t\to\infty} E\varphi(X(t;x)) = \int \varphi(x)d\mu(x) := \varphi^{\mathrm{erg}} \tag{8}$$

for any function $\varphi(x)$ with polynomial growth at infinity (see Refs. 5, 6, 16, and 17 and references therein). Here $X(t;x)$ is the solution $X(t)$ of system (6)-(7) with the initial condition $X(0)=X(0;x)=x$.

It is not difficult to see that the solution of system (6)-(7) preserves the property (4), i.e.,

$$|Q^j(t)| = 1, \quad j=1,\ldots,n \ \text{ for all } \ t \geq 0. \tag{9}$$

System (6)-(7) possesses the Gibbsian stationary measure with the density $\rho(\mathbf{r},\mathbf{p},\mathbf{q},\boldsymbol{\pi})$ from Eq. (5) when the coefficients γ, Γ, g, G, b, and B are such that ρ is a solution of the stationary Fokker–Planck equation corresponding to system (6)-(7). After some calculations, we get the required relations between γ, Γ, g, G, b, and B (see Appendix A). Since numerical methods are usually simpler for systems with additive noise, we limit computational consideration of thermostats in this paper to the case of b_{ii} and B_{ii} both being constant. At the same time, we note that general thermostats defined by Eqs. (6)-(7) may have some beneficial features for certain systems but we leave this question for further study. For constant b_{ii} and B_{ii}, the relations between γ, Γ, g, G, b, and B take the form

$$\gamma g_i(p^j,r^j)=\frac{\beta}{m}\frac{b_{ii}^2}{2}p_i^j \quad \text{and} \quad \Gamma G_i(q^j,\pi^j)=\beta\frac{B_{ii}^2}{2}\frac{\partial H}{\partial \pi_i^j}. \quad (10)$$

In the considered molecular model it is natural to have the same value for all b_{ii}, $i=1,2,3$, and the same value for all B_{ii}, $i=1,\ldots,4$. Further, taking into account the form of Hamiltonian (1), we can write

$$G(q,\pi)=J(q)\pi \quad \text{and} \quad B_{ii}^2=\frac{2M\Gamma}{\beta}$$

with

$$J(q)=\frac{\sum_{l=1}^3 \frac{1}{I_l}S_l q[S_l q]^{\mathsf{T}}}{\sum_{l=1}^3 \frac{1}{I_l}} \quad \text{and} \quad M=\frac{4}{\sum_{l=1}^3 \frac{1}{I_l}}. \quad (11)$$

Note that $\mathrm{Tr}\, J(q)=|q|^2=1$.

Thus, in this paper under *Langevin thermostat* we understand the following stochastic system:

$$dR^j=\frac{P^j}{m}dt, \quad R^j(0)=r^j,$$

$$dP^j=-\nabla_{r^j}U(\mathbf{R},\mathbf{Q})dt-\gamma P^j dt+\sqrt{\frac{2m\gamma}{\beta}}dw^j(t),$$

$$P^j(0)=p^j, \quad (12)$$

$$dQ^j=\sum_{l=1}^3 \nabla_{\pi^j}V_l(Q^j,\Pi^j)dt, \quad Q^j(0)=q^j, \quad |q^j|=1,$$

$$d\Pi^j=-\sum_{l=1}^3 \nabla_{q^j}V_l(Q^j,\Pi^j)dt-\nabla_{q^j}U(\mathbf{R},\mathbf{Q})dt$$

$$-\Gamma J(Q^j)\Pi^j dt+\sqrt{\frac{2M\Gamma}{\beta}}dW^j(t), \quad \Pi^j(0)=\pi^j,$$

$$j=1,\ldots,n, \quad (13)$$

where $J(q)$ and M are from Eq. (11), the rest of the notation is as in Eqs. (6) and (7). We recall that γ and Γ are free parameters having the physical meaning of the strength of coupling to the heat bath.

In Appendix B we also derive the equations for the body-fixed angular velocities ω_x, ω_y, and ω_z corresponding to the rotational Langevin subsystem (13).

B. A mixture of gradient system and Langevin-type equation

Another possibility of stochastic thermostating of Eq. (3) rests on a mixture of a gradient system for the translational dynamics and Langevin-type equation for the rotational dynamics. We note that according to the density of Gibbsian measure (5) the center-of-mass momenta $\mathbf{P}$ are independent Gaussian random variables and they are independent of the other components of the system so we can avoid simulating $\mathbf{P}$ via a differential equation.

Consider the *gradient-Langevin thermostat*,

$$d\mathbf{R}=-\frac{\nu}{m}\nabla_{\mathbf{r}}U(\mathbf{R},\mathbf{Q})dt+\sqrt{\frac{2\nu}{m\beta}}d\mathbf{w}(t), \quad \mathbf{R}(0)=\mathbf{r}, \quad (14)$$

$$dQ^j=\nabla_{\pi^j}\sum_{l=1}^3 V_l(Q^j,\Pi^j)dt, \quad Q^j(0)=q^j, \quad |q^j|=1,$$

$$d\Pi^j=-\nabla_{q^j}\sum_{l=1}^3 V_l(Q^j,\Pi^j)dt-\nabla_{q^j}U(\mathbf{R},\mathbf{Q})dt$$

$$-\Gamma J(Q^j)\Pi^j dt+\sqrt{\frac{2M\Gamma}{\beta}}dW^j(t), \quad \Pi^j(0)=\pi^j,$$

$$j=1,\ldots,n, \quad (15)$$

where all the notation is as in Eqs. (12) and (13) and, in particular, $J(q)$ and M are from Eq. (11). The invariant measure $\rho(\mathbf{r},\mathbf{q},\boldsymbol{\pi})$ [see Eq. (16) below] of system (14)-(15) is Eq. (5) integrated over $\mathbf{p}$. Property (9) is preserved. The gradient-Langevin thermostat has two free parameters, $\nu>0$ and $\Gamma\geq 0$. The latter is the same as in Eq. (13), while the former, measured in units of time, controls the speed of evolution of the gradient subsystem (14).

It is important to note that the gradient system does not have a natural dynamical time evolution similar to Hamiltonian or Langevin dynamics. This is because changing parameter ν simply leads to a time renormalization of the gradient subsystem (14). However, when linked with the Langevin dynamics for rotational degrees of freedom, as in Eqs. (14) and (15), parameter ν controls the "speed" of evolution of the gradient subsystem relative to the speed of the rotational dynamics.

To check that

$$\rho(\mathbf{r},\mathbf{q},\boldsymbol{\pi})\propto\exp\left(-\beta\left[\sum_{j=1}^n\sum_{l=1}^3 V_l(q^j,\pi^j)+U(\mathbf{r},\mathbf{q})\right]\right) \quad (16)$$

is the density of the invariant measure for system (14)-(15), one needs to consider the corresponding stationary Fokker–Planck equation analogously to how it is done in Appendix A for the Langevin-type equations. Let us remark[18] that the gradient subsystem (14) can be viewed as an overdamped limit of the Langevin translational subsystem (12) for a fixed $\mathbf{Q}$.

III. NUMERICAL INTEGRATORS

In this section we consider effective second-order numerical methods for Langevin thermostat (12)-(13) and gradient-Langevin thermostat (14)-(15). We first recall the idea of quasisymplectic integrators for Langevin-type equations introduced in Ref. 19 (see also Refs. 7 and 20) and also some basic facts from stochastic numerics.[20]

Consider the Langevin Eqs. (12) and (13). Let $D_0\in\mathbb{R}^d$, $d=14n$ be a domain with finite volume. The transformation $x=(\mathbf{r}^{\mathsf{T}},\mathbf{p}^{\mathsf{T}},\mathbf{q}^{\mathsf{T}},\pi^{\mathsf{T}})^{\mathsf{T}}\mapsto X(t)=X(t;x)=(\mathbf{R}^{\mathsf{T}}(t;x),\mathbf{P}^{\mathsf{T}}(t;x),\mathbf{Q}^{\mathsf{T}}(t;x),\boldsymbol{\Pi}^{\mathsf{T}}(t;x))^{\mathsf{T}}$ maps D_0 into the domain D_t. The volume V_t of the domain D_t is equal to

$$V_t = \int_{D_t} dX^1, \ldots, dX^d = \int_{D_0} \left| \frac{D(X^1, \ldots, X^d)}{D(x^1, \ldots, x^d)} \right| dx^1, \ldots, dx^d. \quad (17)$$

The Jacobian determinant $\mathbb{J}$ is equal to (see, e.g., Ref. 21),

$$\mathbb{J} = \frac{D(X^1, \ldots, X^d)}{D(x^1, \ldots, x^d)} = \exp(-n(3\gamma + \Gamma)t). \quad (18)$$

System (12)-(13) preserves phase volume when $\gamma=0$ and $\Gamma=0$. If $\gamma \geq 0$ and $\Gamma \geq 0$ with $\gamma\Gamma > 0$ then phase-volume contractivity takes place.

If we omit the damping terms, $-\gamma P^j$ and $-\Gamma J\Pi^j$, in Eqs. (12) and (13) then the system becomes a Hamiltonian system with additive noise,[20,21] i.e., its phase flow preserves symplectic structure. When $\gamma=0$ and $\Gamma=0$, Eqs. (12) and (13) take the form of the deterministic Hamiltonian system (3).

We say that the method based on a one-step approximation $\bar{X}=\bar{X}(t+h;t,x)$, $h>0$, is symplectic if $\bar{X}$ preserves symplectic structure.[20,21] It is natural to expect that making use of numerical methods, which are close, in a sense, to symplectic ones, has advantages when applying to stochastic systems close to Hamiltonian ones. In Ref. 19 (see also Ref. 20) numerical methods (they are called quasisymplectic) for Langevin equations were proposed, which satisfy the two structural conditions:

RL1. *The method applied to Langevin equations degenerates to a symplectic method when the Langevin system degenerates to a Hamiltonian one.*

RL2. *The Jacobian determinant* $\bar{\mathbb{J}}=D\bar{X}/Dx$ does not depend on x.

The requirement RL1 ensures closeness of quasisymplectic integrators to the symplectic ones. As it is always assumed, a method is convergent and, consequently, $\bar{\mathbb{J}}$ is close to $\mathbb{J}$ at any rate. The requirement RL2 is natural since the Jacobian $\mathbb{J}$ of original system (12)-(13) does not depend on x. RL2 reflects the structural properties of the system which are connected with the law of phase-volume contractivity. It is often possible to reach a stronger property consisting in the equality $\bar{\mathbb{J}}=\mathbb{J}$.

We usually consider two types of numerical methods for SDEs: mean-square and weak.[20] Mean-square methods are useful for direct simulation of stochastic trajectories while weak methods are sufficient for evaluation of averages and are simpler than mean-square ones. Therefore, weak methods are most suitable for the purposes of this paper. Let us recall[20] that a method $\bar{X}$ is weakly convergent with order $p>0$ if

$$|E\varphi(\bar{X}(T)) - E\varphi(X(T))| \leq Ch^p, \quad (19)$$

where $h>0$ is a time discretization step and φ is a sufficiently smooth function with growth at infinity not faster than polynomial. The constant C does not depend on h, it depends on the coefficients of a simulated stochastic system, on φ, and T.

A. Numerical schemes for the Langevin thermostat

We assume that system (12)-(13) have to be solved on a time interval $[0,T]$ and for simplicity we use a uniform time discretization with the step $h=T/N$. Using standard ideas of stochastic numerics[19,20] including splitting techniques and the numerical method from Ref. 10 for the deterministic Hamiltonian system (3), we derive two quasisymplectic integrators for Langevin system (12)-(13).

The first integrator (Langevin A) is based on splitting Langevin system (12)-(13) into the Hamiltonian system with additive noise [i.e., Eqs. (12) and (13) without the damping terms] and the deterministic system of linear differential equations of the form

$$\dot{\mathbf{p}} = -\gamma\mathbf{p}, \qquad \dot{\pi}^j = -\Gamma J(q^j)\pi^j, \quad j=1,\ldots,n. \quad (20)$$

We construct a second-order weak quasisymplectic integrator for the stochastic Hamiltonian system[20,21] and appropriately concatenate[19,20] it with the exact solution of Eq. (20). The resulting numerical method is given below.

Introduce the mapping $\Psi_l(t;q,\pi)$: $(q,\pi)\mapsto(\mathcal{Q},\Pi)$ defined by

$$\mathcal{Q} = \cos(\chi_l t)q + \sin(\chi_l t)S_l q, \qquad \Pi = \cos(\chi_l t)\pi + \sin(\chi_l t)S_l \pi, \quad (21)$$

where

$$\chi_l = \frac{1}{4I_l}\pi^{\mathsf{T}} S_l q.$$

The first quasisymplectic scheme for system (12)-(13) can be written in the following form.

Langevin A

$$\mathbf{P}_0 = \mathbf{p}, \quad \mathbf{R}_0 = \mathbf{r}, \quad \mathbf{Q}_0 = \mathbf{q}, \quad \mathbf{\Pi}_0 = \pi,$$

$$\mathcal{P}_{1,k} = \mathbf{P}_k \exp(-\gamma h/2),$$

$$\Pi^j_{1,k} = \exp(-\Gamma J(Q^j_k)h/2)\Pi^j_k, \quad j=1,\ldots,n,$$

$$\mathcal{P}_{2,k} = \mathcal{P}_{1,k} - \frac{h}{2}\nabla_{\mathbf{r}} U(\mathbf{R}_k,\mathbf{Q}_k) + \frac{\sqrt{h}}{2}\sqrt{\frac{2m\gamma}{\beta}}\xi_k,$$

$$\Pi^j_{2,k} = \Pi^j_{1,k} - \frac{h}{2}\nabla_{q^j} U(\mathbf{R}_k,\mathbf{Q}_k) + \frac{\sqrt{h}}{2}\sqrt{\frac{2M\Gamma}{\beta}}\eta^j_k - \frac{h^2}{4}\frac{\Gamma}{\beta}Q^j_k, \quad j=1,\ldots,n,$$

$$\mathbf{R}_{k+1} = \mathbf{R}_k + \frac{h}{m}\mathcal{P}_{2,k},$$

$$(\mathcal{Q}^j_{1,k},\Pi^j_{3,k}) = \Psi_3(h/2;Q^j_k,\Pi^j_{2,k}),$$

$$(\mathcal{Q}^j_{2,k},\Pi^j_{4,k}) = \Psi_2(h/2;\mathcal{Q}^j_{1,k},\Pi^j_{3,k}),$$

$$(\mathcal{Q}^j_{3,k},\Pi^j_{5,k}) = \Psi_1(h;\mathcal{Q}^j_{2,k},\Pi^j_{4,k}),$$

$$(\mathcal{Q}^j_{4,k},\Pi^j_{6,k}) = \Psi_2(h/2;\mathcal{Q}^j_{3,k},\Pi^j_{5,k}),$$

$$(Q^j_{k+1},\Pi^j_{7,k}) = \Psi_3(h/2;\mathcal{Q}^j_{4,k},\Pi^j_{6,k}), \quad j=1,\ldots,n,$$

$$\Pi^j_{8,k} = \Pi^j_{7,k} - \frac{h}{2}\nabla_{q^j}U(\mathbf{R}_{k+1},\mathbf{Q}_{k+1}) + \frac{\sqrt{h}}{2}\sqrt{\frac{2M\Gamma}{\beta}}\eta^j_k - \frac{h^2}{4}\frac{\Gamma}{\beta}Q^j_{k+1}, \quad j=1,\ldots,n,$$

$$\mathcal{P}_{3,k} = \mathcal{P}_{2,k} - \frac{h}{2}\nabla_{\mathbf{r}}U(\mathbf{R}_{k+1},\mathbf{Q}_{k+1}) + \frac{\sqrt{h}}{2}\sqrt{\frac{2m\gamma}{\beta}}\xi_k,$$

$$\mathbf{P}_{k+1} = \mathcal{P}_{3,k}\exp(-\gamma h/2),$$

$$\Pi^j_{k+1} = \exp(-\Gamma J(Q^j_{k+1})h/2)\Pi^j_{8,k}, \quad j=1,\ldots,n,$$

$$k=0,\ldots,N-1, \tag{22}$$

where $\xi_k=(\xi_{1,k},\ldots,\xi_{3n,k})^{\mathbf{T}}$ and $\eta^j_k=(\eta^j_{1,k},\ldots,\eta^j_{4,k})^{\mathbf{T}}$, $j=1,\ldots,n$, with their components being i.i.d. (independent and identically distributed) with the same law,

$$P(\theta=0)=2/3, \quad P(\theta=\pm\sqrt{3})=1/6. \tag{23}$$

It is easy to check[19,20] that scheme (22) is quasisymplectic. Moreover, the Jacobian $\bar{\mathbb{J}}$ of the corresponding one-step approximation is exactly equal to the Jacobian $\mathbb{J}$ of the original system (12)-(13).

To prove the second order of weak convergence of Eqs. (22) and (23), we compared the corresponding one-step approximation with the one-step approximation corresponding to the standard second-order weak method for SDEs with additive noise from Ref. 20 (p. 113). The following properties are used in this proof:

$$2M\sum_{i=0}^{3}\frac{\partial^2}{\partial\pi_i^2}\sum_{l=1}^{3}\nabla_q V_l(q,\pi) = 4q,$$

$$\frac{\partial^2}{\partial\pi_i\partial\pi_j}\nabla_\pi V_l(q,\pi) = 0,$$

and

$$\frac{\partial}{\partial\pi_i^l}V_l(q^j,\pi^j) = \frac{\partial}{\partial q_i^l}V_l(q^j,\pi^j) = 0 \quad \text{for} \quad j\neq l.$$

As it is usual in stochastic numerics,[20] we prove convergence of a numerical method under the global Lipschitz assumption on the coefficients of the stochastic system, which can then be relaxed using the concept of rejecting exploding trajectories.[7]

Analogously to the deterministic case,[10] one can verify that scheme (22) preserves Eq. (9), i.e., $|Q^j_k|=1$, $j=1,\ldots,n$, for all k. We summarize the properties of methods (22)-(23) in the following statement:

Proposition 1. *Numerical scheme* (22)-(23) *for* Eqs. (12) and (13) *is quasisymplectic, it preserves structural property* (9), *and is of weak order two.*

We note that one can choose $\xi_k=(\xi_{1,k},\ldots,\xi_{3n,k})^{\mathbf{T}}$ and $\eta^j_k=(\eta^j_{1,k},\ldots,\eta^j_{4,k})^{\mathbf{T}}$, $j=1,\ldots,n$, so that their components are i.i.d. Gaussian random variables with zero mean and unit variance. In this case the weak order of the scheme remains second as when we use the simple discrete distribution (23). Since simulation of the discrete random variables is cheaper than Gaussian ones, it is preferable to use Eq. (23) and it was used in all our experiments in this paper. Let us remark in passing that in the case of Gaussian random variables the above scheme also converges in the mean-square sense[20] with order one.

Note that $\exp(-\Gamma J(q)h/2)$ in Eq. (22) is the exponent of a matrix. It can be computed using a standard linear algebra package (such as LAPACK). Since $J(q)$ is a symmetric matrix, LAPACK's dsyev routine can be used to obtain the eigendecomposition

$$J(q) = T(q)\Lambda_J(q)T^{\mathbf{T}}(q), \tag{24}$$

where $T(q)$ is a matrix whose columns are the eigenvectors of $J(q)$ and

$$\Lambda_J(q) = \mathrm{diag}(\lambda_{J,1},\ldots,\lambda_{J,4})$$

is a diagonal matrix of the corresponding eigenvalues. Then

$$\exp(-\Gamma J(q)h/2) = T(q)\exp(-\Gamma\Lambda_J(q)h/2)T^{\mathbf{T}}(q),$$

where

$$\exp(-\Gamma\Lambda_J(q)h/2) = \mathrm{diag}(e^{-\Gamma\lambda_{J,1}h/2},\ldots,e^{-\Gamma\lambda_{J,4}h/2}).$$

Alternatively, the matrix exponent $\exp(-\Gamma J(q)h/2)$ in Eq. (22) can be approximated via the Taylor expansion. To ensure the second-order convergence, it is sufficient to approximate it with accuracy $O(h^3)$ at one step; the scheme will remain quasisymplectic but the Jacobian $\bar{\mathbb{J}}$ will no longer be equal to $\mathbb{J}$ in Eq. (18).

When the parameters γ and Γ are large (the strong coupling to the heat bath conditions), we propose to use a numerical integrator for Langevin system (12)-(13) based on the following splitting:

$$d\mathbf{P}_I = -\gamma\mathbf{P}_I dt + \sqrt{\frac{2m\gamma}{\beta}}d\mathbf{w}(t),$$

$$d\Pi^j_I = -\Gamma J(q)\Pi^j_I dt + \sqrt{\frac{2M\Gamma}{\beta}}dW^j(t), \tag{25}$$

$$d\mathbf{R}_{II} = \frac{\mathbf{P}_{II}}{m}dt,$$

$$d\mathbf{P}_{II} = -\nabla_{\mathbf{r}}U(\mathbf{R}_{II},\mathbf{Q}_{II})dt,$$

$$dQ^j_{II} = \nabla_{\pi^j}\sum_{l=1}^{3}V_l(Q^j_{II},\Pi^j_{II})dt,$$

$$d\Pi^j_{II} = -\nabla_{q^j}U(\mathbf{R}_{II},\mathbf{Q}_{II})dt - \nabla_{q^j}\sum_{l=1}^{3}V_l(Q^j_{II},\Pi^j_{II})dt,$$

$$j=1,\ldots,n. \tag{26}$$

SDEs (25) have the exact solution,

$$\mathbf{P}_I(t) = \mathbf{P}_I(0)e^{-\gamma t} + \sqrt{\frac{2m\gamma}{\beta}}\int_0^t e^{-\gamma(t-s)}d\mathbf{w}(s),$$

$$\Pi_I^j(t) = \exp(-\Gamma J(q)t)\Pi_I^j(0) + \sqrt{\frac{2M\Gamma}{\beta}}\int_0^t \exp(-\Gamma J(q)(t-s))dW^j(s). \quad (27)$$

To construct a method based on splitting (25)-(26), we take half a step of Eq. (25) using Eq. (27), one step of a symplectic method for Eq. (26), and again half a step of Eq. (25).

The Ito integral in the expression for Π_I^j in Eq. (27) is a four-dimensional Gaussian vector with zero mean and the covariance matrix

$$C(t;q) = \frac{2M\Gamma}{\beta}\int_0^t \exp[-2\Gamma J(q)(t-s)]ds = \frac{M}{\beta}T(q)\Lambda_C(t;q,\Gamma)T^{\mathsf{T}}(q), \quad (28)$$

where $T(q)$ is as in Eq. (24) and

$$\Lambda_C(t;q,\Gamma) = \mathrm{diag}(\lambda_{C,1},\ldots,\lambda_{C,4})$$

with

$$\lambda_{C,i}(t;q,\Gamma) = \begin{cases} 2\Gamma t & \text{if } \lambda_{J,i}=0, \\ \dfrac{1-\exp(-2\Gamma\lambda_{J,i}(q)t)}{\lambda_{J,i}(q)} & \text{otherwise.} \end{cases}$$

$$i = 1,\ldots,4. \quad (29)$$

We note that at least one eigenvalue of $J(q)$ equals zero by definition.

Finally, introduce a 4×4-dimensional matrix $\sigma(t,q)$ such that

$$\sigma(t;q)\sigma^{\mathsf{T}}(t;q) = C(t;q). \quad (30)$$

Since $C(t;q)$ is a symmetric matrix, $\sigma(t;q)$ can be determined as a lower triangular matrix in the Cholesky decomposition of $C(t;q)$. LAPACK's dpotrf can be used for this purpose.

With the above definitions, we obtain the following quasisymplectic scheme for system (12)-(13).

Langevin B

$$\mathbf{P}_0 = \mathbf{p}, \quad \mathbf{R}_0 = \mathbf{r}, \quad \mathbf{Q}_0 = \mathbf{q}, \quad \mathbf{\Pi}_0 = \pi,$$

$$\mathcal{P}_{1,k} = \mathbf{P}_k e^{-\gamma h/2} + \sqrt{\frac{m}{\beta}(1-e^{-\gamma h})}\xi_k,$$

$$\Pi_{1,k}^j = \exp(-\Gamma J(Q_k^j)h/2)\Pi_k^j + \sigma(h/2;Q_k^j)\eta_k^j, \quad j=1,\ldots,n,$$

$$\mathcal{P}_{2,k} = \mathcal{P}_{1,k} - \frac{h}{2}\nabla_{\mathbf{r}}U(\mathbf{R}_k,\mathbf{Q}_k),$$

$$\Pi_{2,k}^j = \Pi_{1,k}^j - \frac{h}{2}\nabla_{q^j}U(\mathbf{R}_k,\mathbf{Q}_k), \quad j=1,\ldots,n,$$

$$\mathbf{R}_{k+1} = \mathbf{R}_k + \frac{h}{m}\mathcal{P}_{2,k},$$

$$(\mathcal{Q}_{1,k}^j,\Pi_{3,k}^j) = \Psi_3(h/2;\mathcal{Q}_k^j,\Pi_{2,k}^j),$$

$$(\mathcal{Q}_{2,k}^j,\Pi_{4,k}^j) = \Psi_2(h/2;\mathcal{Q}_{1,k}^j,\Pi_{3,k}^j),$$

$$(\mathcal{Q}_{3,k}^j,\Pi_{5,k}^j) = \Psi_1(h;\mathcal{Q}_{2,k}^j,\Pi_{4,k}^j),$$

$$(\mathcal{Q}_{4,k}^j,\Pi_{6,k}^j) = \Psi_2(h/2;\mathcal{Q}_{3,k}^j,\Pi_{5,k}^j),$$

$$(\mathcal{Q}_{k+1}^j,\Pi_{7,k}^j) = \Psi_3(h/2;\mathcal{Q}_{4,k}^j,\Pi_{6,k}^j), \quad j=1,\ldots,n,$$

$$\Pi_{8,k}^j = \Pi_{7,k}^j - \frac{h}{2}\nabla_{q^j}U(\mathbf{R}_{k+1},\mathbf{Q}_{k+1}), \quad j=1,\ldots,n,$$

$$\mathcal{P}_{3,k} = \mathcal{P}_{2,k} - \frac{h}{2}\nabla_{\mathbf{r}}U(\mathbf{R}_{k+1},\mathbf{Q}_{k+1}),$$

$$\mathbf{P}_{k+1} = \mathcal{P}_{3,k}e^{-\gamma h/2} + \sqrt{\frac{m}{\beta}(1-e^{-\gamma h})}\zeta_k,$$

$$\Pi_{k+1}^j = \exp(-\Gamma J(Q_{k+1}^j)h/2)\Pi_{8,k}^j + \sigma(h/2;Q_{k+1}^j)\varsigma_k^j, \quad j=1,\ldots,n, \quad k=0,\ldots,N-1, \quad (31)$$

where $\xi_k=(\xi_{1,k},\ldots,\xi_{3n,k})^{\mathsf{T}}$, $\zeta_k=(\zeta_{1,k},\ldots,\zeta_{3n,k})^{\mathsf{T}}$, and $\eta_k^j=(\eta_{1,k}^j,\ldots,\eta_{4,k}^j)^{\mathsf{T}}$, $\varsigma_k^j=(\varsigma_{1,k}^j,\ldots,\varsigma_{4,k}^j)^{\mathsf{T}}$, $j=1,\ldots,n$, with their components being i.i.d. with the same law (23).

As in the case of scheme (22)-(23), the Jacobian $\bar{\mathbb{J}}$ of the one-step approximation corresponding to integrator (31)-(23) is exactly equal to the Jacobian $\mathbb{J}$ of the original system (12)-(13). The following proposition can be proved.

Proposition 2. *The numerical scheme* (31)-(23) *for* system (12)-(13) *is quasisymplectic, it preserves the structural property* (9), *and is of weak order two.*

We note that if we omit the rotational component in system (12)-(13), scheme (22)-(23) coincides with a second-order weak quasisymplectic method from Ref. 19 (see also Refs. 7 and 20) and scheme (31)-(23) is close to the one from Ref. 3 (see also Refs. 4, 19, 20, and 22). Both stochastic integrators (22)-(23) and (31)-(23) degenerate to the deterministic scheme from Ref. 10 when $\gamma=0$ and $\Gamma=0$. Scheme (31)-(23) is usually preferable when γ and/or Γ are large (see our experimental results in Sec. IV and a discussion in the case of translational Langevin equations in Ref. 22). It is slightly more expensive than system (22)-(23) due to the need of generating the additional $7n$ random variables $\zeta_{i,k}$ and ς_k^j per step and computing Cholesky factorization. However, for most molecular system of practical interest in computational chemistry and physics, where majority of the computational effort is spent on force calculations, the additional cost is negligible.

B. Numerical scheme for the gradient-Langevin system

To construct the numerical scheme for the gradient-Langevin system (14)-(15), we exploit the Runge–Kutta method of order two for equations with additive noise from Ref. 20 (p. 113) to simulate the "gradient" part (14), while the "Langevin" rotational part (15) is approximated in the same way as in Eq. (31). The resulting second-order weak scheme has the form.

Gradient-Langevin

$$\mathbf{R}_0 = \mathbf{r}, \quad \mathbf{Q}_0 = \mathbf{q}, \quad \mathbf{\Pi}_0 = \pi,$$

$$\Pi^j_{1,k} = \exp(-\Gamma J(Q^j_k)h/2)\Pi^j_k + \sigma(h/2;Q^j_k)\,\eta^j_k,$$

$$j = 1, \ldots, n,$$

$$\Delta R_k = -\frac{h}{2}\frac{\nu}{m}\nabla_{\mathbf{r}} U(\mathbf{R}_k, \mathbf{Q}_k) + \frac{\sqrt{h}}{2}\sqrt{\frac{2\nu}{m\beta}}\xi_k,$$

$$\mathcal{R}_k = \mathbf{R}_k + 2 \times \Delta R_k,$$

$$\Pi^j_{2,k} = \Pi^j_{1,k} - \frac{h}{2}\nabla_{q^j} U(\mathbf{R}_k, \mathbf{Q}_k), \quad j = 1, \ldots, n,$$

$$(\mathcal{Q}^j_{1,k}, \Pi^j_{3,k}) = \Psi_3(h/2; Q^j_k, \Pi^j_{2,k}),$$

$$(\mathcal{Q}^j_{2,k}, \Pi^j_{4,k}) = \Psi_2(h/2; \mathcal{Q}^j_{1,k}, \Pi^j_{3,k}),$$

$$(\mathcal{Q}^j_{3,k}, \Pi^j_{5,k}) = \Psi_1(h; \mathcal{Q}^j_{2,k}, \Pi^j_{4,k}),$$

$$(\mathcal{Q}^j_{4,k}, \Pi^j_{6,k}) = \Psi_2(h/2; \mathcal{Q}^j_{3,k}, \Pi^j_{5,k}),$$

$$(Q^j_{k+1}, \Pi^j_{7,k}) = \Psi_3(h/2; \mathcal{Q}^j_{4,k}, \Pi^j_{6,k}), \quad j = 1, \ldots, n,$$

$$\mathbf{R}_{k+1} = \mathcal{R}_k - \Delta R_k + \frac{\sqrt{h}}{2}\sqrt{\frac{2\nu}{m\beta}}\xi_k - \frac{h}{2}\frac{\nu}{m}\nabla_{\mathbf{r}} U(\mathcal{R}_k, \mathbf{Q}_{k+1}),$$

$$\Pi^j_{8,k} = \Pi^j_{7,k} - \frac{h}{2}\nabla_{q^j} U(\mathbf{R}_{k+1}, \mathbf{Q}_{k+1}),$$

$$\Pi^j_{k+1} = \exp(-\Gamma J(Q^j_{k+1})h/2)\Pi^j_{8,k} + \sigma(h/2;Q^j_{k+1})\varsigma^j_k,$$

$$j = 1, \ldots, n; \quad k = 0, \ldots, N-1, \tag{32}$$

where $\xi_k = (\xi_{1,k}, \ldots, \xi_{3n,k})^{\mathsf{T}}$ and $\eta^j_k = (\eta^j_{1,k}, \ldots, \eta^j_{4,k})^{\mathsf{T}}$, $\varsigma^j_k = (\varsigma^j_{1,k}, \ldots, \varsigma^j_{4,k})^{\mathsf{T}}$, $j = 1, \ldots, n$, with their components being i.i.d. with the same law (23). The following proposition can be proved.

Proposition 3. Numerical scheme (32)-(23) for Eqs. (14) and (15) preserves the structural property (9) and is of weak order two.

We draw attention to the fact that the above gradient-Langevin scheme requires two force calculations per step and thus is approximately twice as expensive as the Langevin schemes presented in Sec. III A.

C. Computational errors

Let us recall that the objective is to compute highly multidimensional integrals with respect to the Gibbsian measure $\mu(x)$ with density (5). The considered stochastic systems (12)-(13) and (14)-(15) are assumed to be ergodic with the Gibbsian invariant measure and we can represent the integrals of interest as [cf. Eq. (8)],

$$\varphi^{\text{erg}} = \int \varphi(x)d\mu(x) = \lim_{t\to\infty} E\varphi(X(t;x)). \tag{33}$$

We are interested here in systems solutions of which satisfy a stronger condition, namely they are exponentially ergodic, i.e., for any $x \in \mathbb{R}^{14n}$ and any function φ with a polynomial growth,

$$|E\varphi(X(t;x)) - \varphi^{\text{erg}}| \le Ce^{-\lambda t}, \quad t \ge 0, \tag{34}$$

where $C > 0$ and $\lambda > 0$ are some constants. In Refs. 5, 6, and 17 (see also references therein), one can find conditions under which Langevin equations are exponentially ergodic.

It follows from Eq. (34) [and Eq. (33)] that for any $\varepsilon > 0$ there exists $T_0 > 0$ such that for all $T \ge T_0$,

$$|E\varphi(X(T;x)) - \varphi^{\text{erg}}| \le \varepsilon. \tag{35}$$

Then we can use the following estimate for the ergodic limit φ^{erg},

$$\varphi^{\text{erg}} \approx E\varphi(X(T;x)) \approx E\varphi(\bar{X}(T;x)) \approx \hat{\varphi}^{\text{erg}} := \frac{1}{L}\sum_{l=1}^{L} \varphi(\bar{X}^{(l)}(T;x)), \tag{36}$$

where T is a sufficiently large time, $\bar{X}$ is an approximation of X, and L is the number of independent approximate realizations. The total error

$$R_{\hat{\varphi}^{\text{erg}}} := \hat{\varphi}^{\text{erg}} - \varphi^{\text{erg}} \tag{37}$$

consists of three parts: the error ε of the approximation φ^{erg} by $E\varphi(X(T;x))$, the error of numerical integration Ch^p [see Eq. (19)], and the Monte Carlo error; i.e.,

$$R_{\hat{\varphi}^{\text{erg}}} \sim Ch^p + \varepsilon + O\left(\frac{1}{\sqrt{L}}\right),$$

or more specifically

$$\text{bias}(\hat{\varphi}^{\text{erg}}) = |E\hat{\varphi}^{\text{erg}} - \varphi^{\text{erg}}| \le Ch^p + \varepsilon,$$

$$\text{var}(\hat{\varphi}^{\text{erg}}) = O(1/L).$$

Each error is controlled by its own parameter: sufficiently large T ensures smallness of the error $|\varphi^{\text{erg}} - E\varphi(X(T;x))|$; time step h (as well as the choice of numerical method) controls the numerical integration error; the statistical error is regulated by choosing an appropriate number of independent trajectories L.

The other, commonly used in molecular dynamics, numerical approach to calculating ergodic limits is based on the known equality

$$\lim_{t\to\infty}\frac{1}{t}\int_0^t \varphi(X(s;x))ds = \varphi^{\mathrm{erg}}\ a\ .\ s\ .\ , \tag{38}$$

where the limit does not depend on x. Then by approximating a single trajectory, one gets the following estimator for φ^{erg},

$$\varphi^{\mathrm{erg}} \sim \frac{1}{\tilde{T}}\int_0^{\tilde{T}} \varphi(X(s;x))ds \sim \check{\varphi}^{\mathrm{erg}} := \frac{1}{L}\sum_{l=1}^{L} \varphi(\bar{X}(lh;x)), \tag{39}$$

where $\tilde{T}$ is sufficiently large and $Lh=\tilde{T}$. In Ref. 23 this approach was rigorously justified in the case of ergodic SDEs with nondegenerate noise and globally Lipschitz coefficients. Let us emphasize that $\tilde{T}$ in Eq. (39) is much larger than T in Eqs. (35) and (36) because $\tilde{T}$ should be such that it not just ensures the distribution of $X(t)$ to be close to the invariant distribution (like it is required from T) but it should also guarantee smallness of variance of $\check{\varphi}^{\mathrm{erg}}$. See further details concerning computing ergodic limits in Ref. 7 and references therein.

IV. NUMERICAL INVESTIGATION

In this section we present a numerical study of the Langevin and gradient-Langevin thermostats derived in Sec. II. The overall performance of a thermostat algorithm depends both on the choice of the thermostat (i.e., of continuous dynamics which produce the exact sample from the canonical distribution) and quality of a numerical scheme (i.e., approximate discrete dynamics) used. Accordingly, the investigation here is split into two parts: (i) analysis of the proposed stochastic thermostats from Sec. II (continuous dynamics) and (ii) analysis of the proposed numerical integrators from Sec. III for these thermostats. In particular, we investigate the dependence of the thermostat properties on the choice of parameters γ and Γ for Langevin system (12)-(13) and ν and Γ for the gradient-Langevin system (14)-(15), as well as the dependence of the numerical discretization errors of the numerical schemes Langevin A, Langevin B, and gradient-Langevin on the integration step size h. Our practical recommendations on which algorithm is preferable are based on the combined outcomes from these two parts of our numerical study.

As a model system, we use the popular TIP4P rigid model of water.[11] In order to speed up the simulations, both Lennard-Jones and electrostatic interactions are smoothly turned off between 9.5 and 10 Å. This truncation has minimal effect on the structure of liquid water, but leads to a lower estimated melting temperature[24] of 219 K.

The two key requirements of a thermostat are as follows: (i) correct sampling of phase space points distributed according to the Gibbs distribution at a desired thermostat temperature T, and (ii) rapid relaxation of the system to the desired equilibrium state. The numerical accuracy of the sampling can be estimated by comparing the values of various system properties (e.g., kinetic and potential energies, pressure) averaged over long simulation runs to those obtained with a much smaller step size h.

To estimate how quickly the system relaxes to the desired equilibrium state we use the following simple experiment. A system of 2000 TIP4P water molecules is equilibrated at $T_0=220$ K. Then the temperature of the thermostat is increased (instantaneously) to $T_1=270$ K, and the run is continued until the system is equilibrated at the new temperature. We deliberately choose to simulate the system at lower temperatures (close to the melting temperature for this model of water), where the relaxation of the system is expected to be slower.

Assuming that the system is exponentially ergodic [see Eq. (34)], we can expect that any measured quantity A will relax from its equilibrium value A_0 at T_0 to the equilibrium value A_1 at T_1 according to the approximate formula

$$EA(t) \equiv \langle A(t)\rangle \doteq A_1 + (A_0 - A_1)\exp(-t/\tau_A), \tag{40}$$

where τ_A is the characteristic relaxation time of the quantity A. The temperature switch occurs at $t=0$ and the angle brackets denote average over an ensemble of independent simulation runs. The subscript on τ_A indicates that different quantities may relax with different rates. The rate of system equilibration should be estimated from the *maximum* value of τ_A among the quantities of interest.

The quantities we measure include the translational kinetic temperature

$$\mathcal{T}_{\mathrm{tr}} = \frac{\mathbf{p}^{\mathsf{T}}\mathbf{p}}{3nk_B m}, \tag{41}$$

rotational kinetic temperature

$$\mathcal{T}_{\mathrm{rot}} = \frac{2}{3nk_B}\sum_{j=1}^{n}\sum_{l=1}^{3} V_l(q^j,\pi^j), \tag{42}$$

and potential energy per molecule

$$\mathcal{U} = \frac{1}{n}U(\mathbf{r},\mathbf{q}). \tag{43}$$

To illustrate the response of the system to the instantaneous temperature change, we show in Fig. 1 the result of applying the Langevin thermostat only to the translational degrees of freedom, i.e., $\Gamma=0$ in Eq. (13). As expected, the translational kinetic temperature quickly relaxes to the new temperature, while the rotational kinetic temperature and potential energy lag behind. To estimate the relaxation rates of the measured quantities, we use the least-squares fit of the exponential function (40) to the average measured quantity $\langle A(t)\rangle$.

In all the simulations we performed, the potential energy relaxation time is larger than that for either of the kinetic temperatures. Therefore, we determine the relaxation time of the system to the new equilibrium state based on the value of $\tau_{\mathcal{U}}$.

Varying the value of the translational Langevin parameter γ, we observe that relaxation is slower for both small and large values of γ, with the fastest relaxation around $\gamma=4.0\ \mathrm{ps}^{-1}$. The existence of an optimal value for the choice of the thermostat parameter is consistent with observations in Ref. 22 and can be understood in terms of the interaction of the system with the thermostat. For small values of γ, the

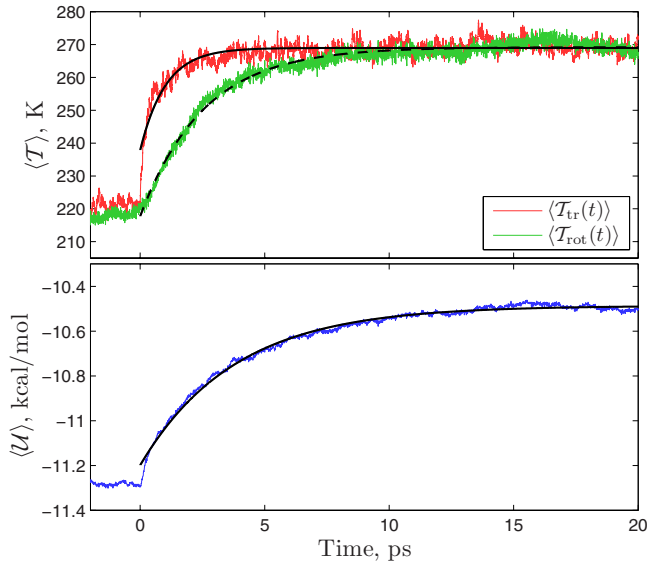

FIG. 1. (Color online) Relaxation dynamics with translational Langevin thermostat: $\gamma=4.0$ ps^{-1}, $\Gamma=0$. Thin lines show relaxation dynamics averaged over ten independent runs, thick lines (solid and dashed for translational and rotational temperatures, respectively) show the least-squares fit to formula (40). The estimated values of the relaxation times are $\tau_{\mathcal{T}_{\rm tr}}=0.2$ ps, $\tau_{\mathcal{T}_{\rm rot}}=1.9$ ps, and $\tau_{\mathcal{U}}=3.6$ ps.

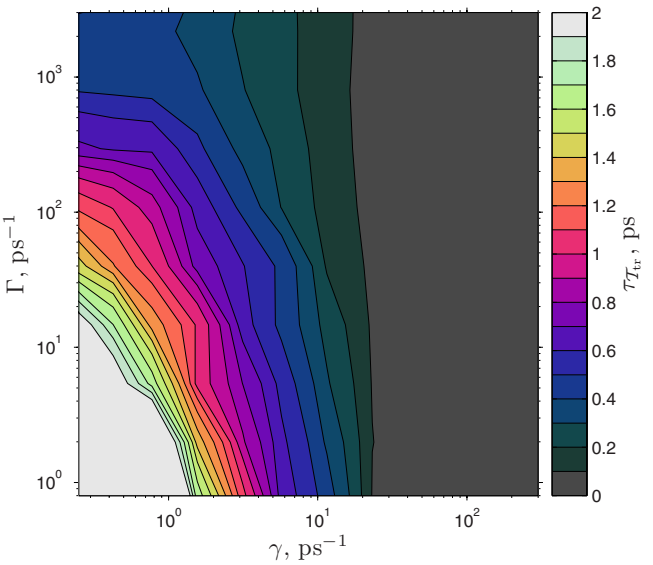

FIG. 2. (Color online) Translational temperature relaxation time for the Langevin thermostat (12)-(13) as a function of the thermostat parameters γ and Γ.

relaxation of the system is slow due to the limited heat flux between the system and the thermostat. For large γ, even though the kinetic temperature relaxes very quickly, the relaxation of the configurational state of the system is apparently hindered by the disruptive influence of the random force on the Hamiltonian dynamics which is driving the system to the new equilibrium.

A. Langevin thermostats

Next, we investigate the dependence of the system relaxation time τ_A on both γ and Γ in Eqs. (12) and (13). In order to minimize the influence of the numerical discretization error, we use a relatively small time step of 0.2 fs. With such a small time step, the difference between Langevin A and Langevin B is negligible compared to the sampling error. To produce the results reported below, we use Langevin A. We evaluate $\tau_{\mathcal{U}}$ on a logarithmic grid of γ (ranging from 0.2 to 300 ps^{-1}) and Γ (ranging from 0.8 to 3000 ps^{-1}) values using five independent runs at each point. The results are shown in Figs. 2–4. As expected, the relaxation speed of translational and rotational temperatures uniformly increases with increasing values of γ and Γ, respectively. At the same time, the relaxation speed of the potential energy exhibits nonuniform dependence on the thermostat parameters. As can be seen in Fig. 4, the fastest relaxation of the system is achieved when the Langevin thermostat is applied to both translational and rotational degrees of freedom, with $\gamma=2-8$ ps^{-1} and $\Gamma=3-40$ ps^{-1}. The relaxation dynamics of the system with the "optimal" choice of Langevin thermostat parameters is demonstrated in Fig. 5. In this case $\tau_{\mathcal{T}_{\rm tr}}=0.28$ ps, $\tau_{\mathcal{T}_{\rm rot}}=0.26$ ps, and $\tau_{\mathcal{U}}=2.0$ ps, which show that the system relaxation is almost twice as fast as when the Langevin thermostat is applied only to translational degrees of freedom. Note that the results shown in Fig. 4 for γ larger than about 100 ps^{-1} or Γ larger than about 1000 ps^{-1} are not reliable due to excessive coupling of the system to the thermostat, which disrupts the Hamiltonian flow of the system. In this case, the relaxation dynamics is poorly represented by the exponential function (40) and thus the fits produce misleading values for the system relaxation time.

In order to further investigate the properties of the Langevin thermostat, we have also computed the integrated autocorrelation time for the measured quantities of the system equilibrated at 270 K,

$$\bar{\tau}_A = \int_0^\infty R_A(t)dt,$$

where

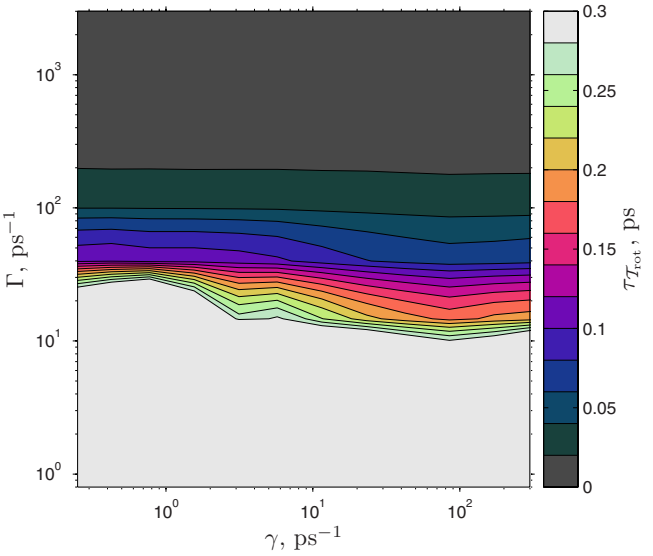

FIG. 3. (Color online) Rotational temperature relaxation time for the Langevin thermostat (12)-(13) as a function of the thermostat parameters γ and Γ.

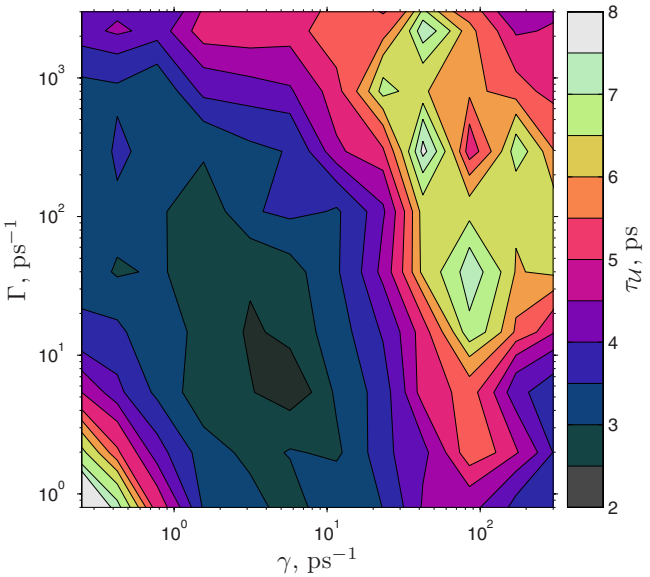

FIG. 4. (Color online) Potential energy relaxation time for the Langevin thermostat (12)-(13) as a function of the thermostat parameters γ and Γ.

$$R_A(t) = E[(A(t') - \mu_A)(A(t'+t) - \mu_A)]/\sigma_A^2$$

is the time autocorrelation function for the quantity A with μ_A and σ_A^2 being the estimated mean and variance of A, respectively. In order to obtain sufficiently accurate results for the integrated autocorrelation time, especially for $\bar{\tau}_{\mathcal{U}}$, we used 500 ps runs, which were much longer than the 20 ps runs used to estimate the relaxation times τ_A. Therefore, we computed $\bar{\tau}_A$ at a few values of parameters γ and Γ. The results, presented in Table I, illustrate that the dependence of $\bar{\tau}_A$ on the thermostat parameters is similar to that of the relaxation time τ_A: while $\bar{\tau}_{\mathcal{T}_{\rm tr}}$ and $\bar{\tau}_{\mathcal{T}_{\rm rot}}$ decrease with increasing

TABLE I. Integrated autocorrelation times for translational and rotational kinetic temperatures and potential energy of the system with Langevin thermostat equilibrated at 270 K.

γ (ps^{-1})	Γ (ps^{-1})	$\bar{\tau}_{\mathcal{T}_{\rm tr}}$ (ps)	$\bar{\tau}_{\mathcal{T}_{\rm rot}}$ (ps)	$\bar{\tau}_{\mathcal{U}}$ (ps)
0.211	0.731	1.037	1.019	6.08
0.573	1.987	0.461	0.481	3.00
1.558	5.400	0.169	0.201	1.48
4.234	14.68	0.092	0.086	1.78
11.51	39.90	0.048	0.039	1.99
31.29	108.5	0.014	0.017	3.15

γ and Γ, $\bar{\tau}_{\mathcal{U}}$ reaches a minimum at approximately the same values of γ and Γ as the relaxation time $\tau_{\mathcal{U}}$.

Now we look at the performance of the numerical integrators proposed in Sec. III A for Langevin thermostat (12)-(13). Since both Langevin A and B are second-order methods, the calculated average quantities for simulations with step size h should have the form[20,25]

$$\langle A\rangle_h = \langle A\rangle_0 + C_A h^2 + O(h^3), \tag{44}$$

where $\langle A\rangle_h$ denotes the average value of dynamical quantity $A(t)$ calculated over a numerical trajectory with time step h. The dependence of $\langle \mathcal{T}_{\rm tr}\rangle_h$, $\langle \mathcal{T}_{\rm rot}\rangle_h$, and $\langle \mathcal{U}\rangle_h$ on h for both Langevin A and B is illustrated in Fig. 6. It appears that Langevin A has larger discretization error for the rotational temperature and smaller error for the potential energy than Langevin B, which makes Langevin A better for evaluating potential energy for this system. The linear dependence of the measured quantities on h^2 is maintained up to a relatively large time step of about $h=7$ fs. The values of the slopes C_A are listed in Table II. Both methods become unstable at about $h=10$ fs.

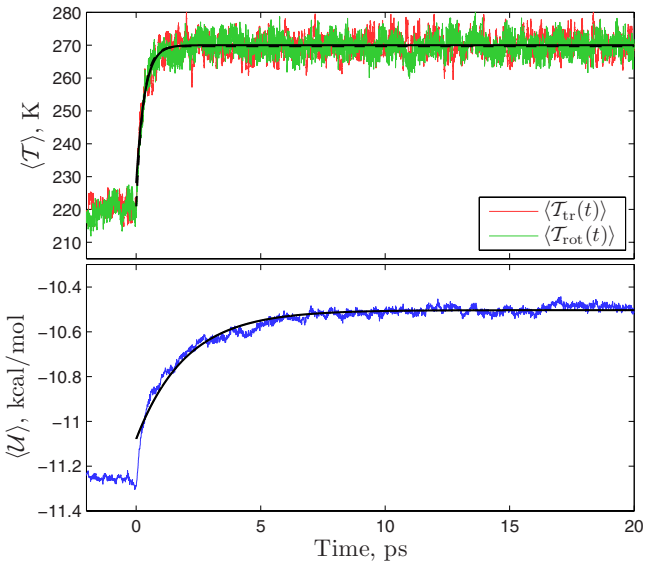

FIG. 5. (Color online) Relaxation dynamics with optimal choice of Langevin thermostat parameters: $\gamma=4.0$ ps^{-1}, $\Gamma=10.0$ ps^{-1}. Thin lines show relaxation dynamics averaged over ten independent runs, thick lines (solid and dashed for translational and rotational temperatures, respectively) show the least-squares fit to formula (40). The estimated values of the relaxation times are $\tau_{\mathcal{T}_{\rm tr}}=0.28$ ps, $\tau_{\mathcal{T}_{\rm rot}}=0.26$ ps, and $\tau_{\mathcal{U}}=2.0$ ps.

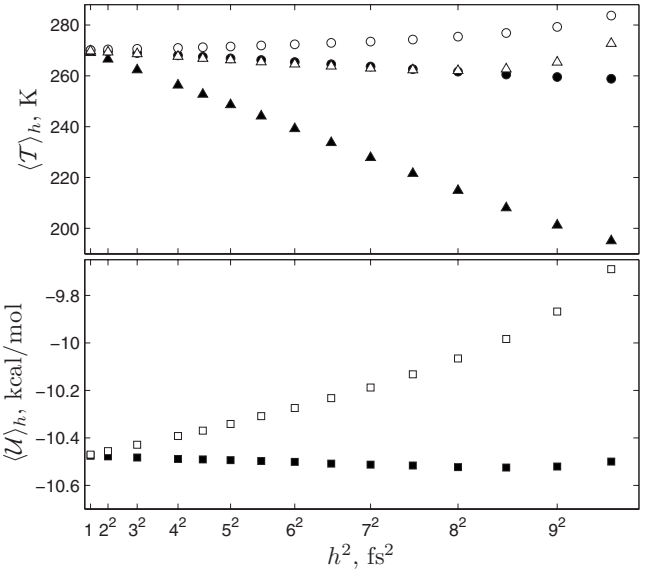

FIG. 6. Dependence of the approximated average properties of a system of 2000 TIP4P water molecules on the integration time step h for Langevin A and B. The system is equilibrated with the thermostat parameters $\gamma=4.0$ ps^{-1}, $\Gamma=10.0$ ps^{-1}, and $T=270$ K. The quantities $\langle \mathcal{T}_{\rm tr}\rangle_h$, $\langle \mathcal{T}_{\rm rot}\rangle_h$, and $\langle \mathcal{U}\rangle_h$ are denoted by circles, triangles, and squares, respectively. Solid and open symbols refer to Langevin A and B, respectively.

TABLE II. Values of the coefficients C_A in the discretization errors (44) for the measured quantities with Langevin A and B. The system parameters are as in Fig. 6.

	Langevin A	Langevin B
$C_{\mathcal{T}_{\rm tr}}$, K/fs^2	−0.13	0.06
$C_{\mathcal{T}_{\rm rot}}$, K/fs^2	−0.85	−0.14
$C_{\mathcal{U}}$, kcal/mol fs^2	−0.0007	0.0056

We have investigated the dependence of $\langle A\rangle_0$ and C_A on the thermostat parameters γ and Γ, by running simulations with time steps $h=2$ and 3 fs and estimating these quantities from the straight line fit with respect to h^2. We consider the fit to be justified if the higher order terms in Eq. (44) are small, i.e., when the quantities $\langle\mathcal{T}_{\rm tr}\rangle_0$ and $\langle\mathcal{T}_{\rm rot}\rangle_0$ determined from Eq. (44) are equal to the thermostat temperature parameter $T=270$ K. In Fig. 7 we show results for the translational temperature measurements in simulations with Langevin A and B. As expected, $\langle\mathcal{T}_{\rm tr}\rangle_0$ converges to 270 K. We note in passing that smaller statistical errors are observed at larger values of γ. The behavior of $C_{\mathcal{T}_{\rm tr}}$ for Langevin A exhibits a plateau for small and moderate values of γ and Γ and then changes rapidly at values that are "too large" for this system. By contrast, the translational temperature discretization error of Langevin B thermostat exhibits consistent behavior for all values of γ and Γ. Similar differences between Langevin A and B can be seen in the measurements of rotational temperature and potential energy shown in Figs. 8 and 9, respectively. As can be seen from the plot of $\langle\mathcal{T}_{\rm rot}\rangle_0$ in Fig. 8, the straight line fit also breaks down at large Γ values in Langevin A.

B. Gradient-Langevin thermostat

Here we describe numerical experiments with the gradient-Langevin thermostat (14)-(15) introduced in Sec. II B. Since the gradient system for the translational motion does not include linear momenta **P**, the translational kinetic temperature $\mathcal{T}_{\rm tr}$ is not available for measurement in this case. Therefore, in our numerical experiments we measure the rotational temperature $\mathcal{T}_{\rm rot}$ and potential energy per particle $\mathcal{U}$ as defined by Eqs. (42) and (43), respectively.

For the particular system studied here, the gradient-Langevin numerical scheme (32)-(23) from Sec. III B becomes unstable when the product $h\nu$ is larger than about 200 fs^2. Therefore, with the step size of $h=0.2$ fs used in our simulations, we can study the properties of the gradient-Langevin scheme with ν up to about 1000 fs.

We conducted the relaxation experiment, where we monitored $\langle\mathcal{T}_{\rm rot}(t)\rangle$ and $\langle\mathcal{U}(t)\rangle$ while the thermostat temperature parameter was switched from 220 to 270 K. The relaxation times $\tau_{\mathcal{T}_{\rm rot}}$ and $\tau_{\mathcal{U}}$ for these quantities were calculated for different values of ν and Γ. The results are shown in Figs. 10 and 11. As expected, the relaxation time for rotational temperature decreases with increasing value of Γ. The some-

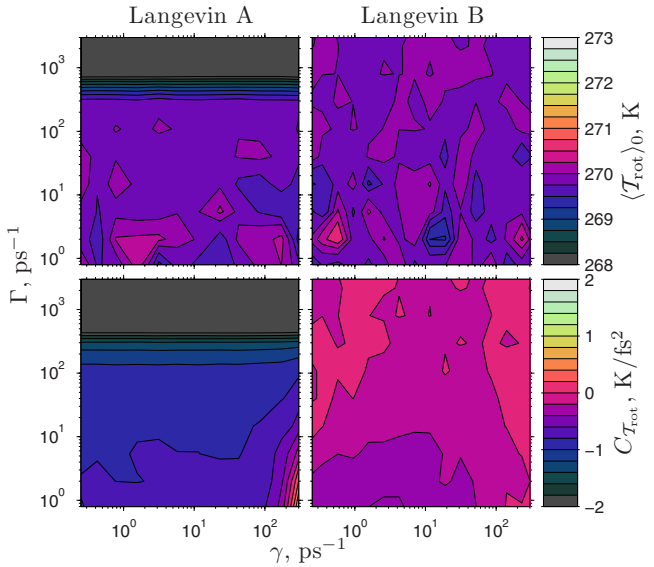

FIG. 8. (Color online) Dependence of $\langle\mathcal{T}_{\rm rot}\rangle_0$ and $C_{\mathcal{T}_{\rm rot}}$ on γ and Γ for Langevin A and B.

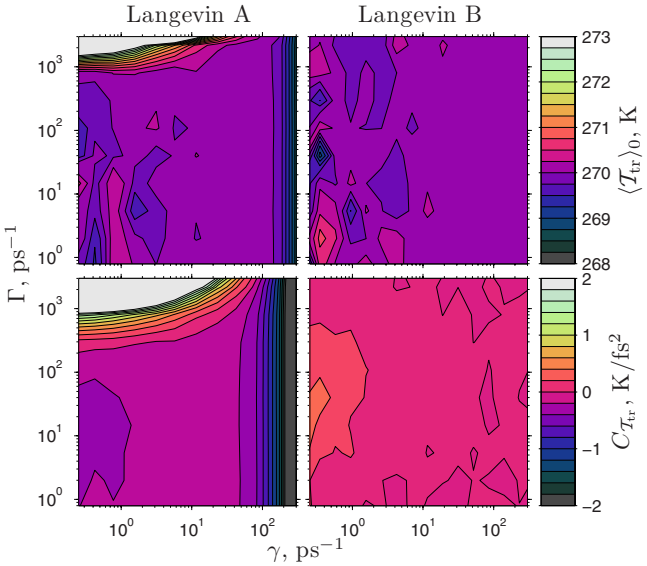

FIG. 7. (Color online) Dependence of $\langle\mathcal{T}_{\rm tr}\rangle_0$ and $C_{\mathcal{T}_{\rm tr}}$ on γ and Γ for Langevin A and B.

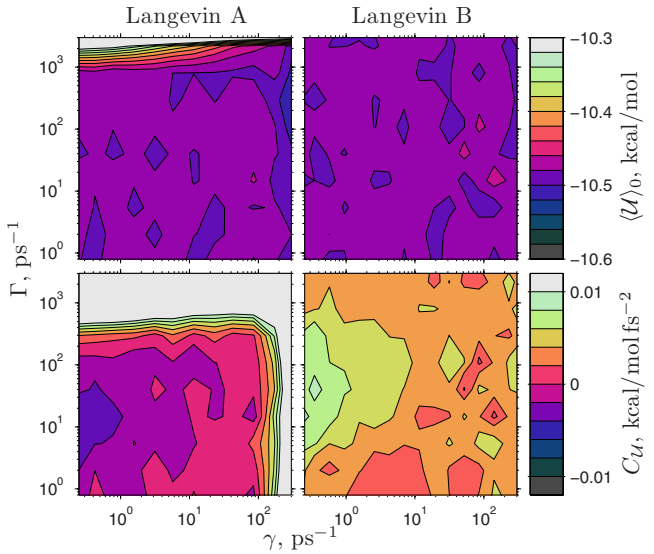

FIG. 9. (Color online) Dependence of $\langle\mathcal{U}\rangle_0$ and $C_{\mathcal{U}}$ on γ and Γ for Langevin A and B.

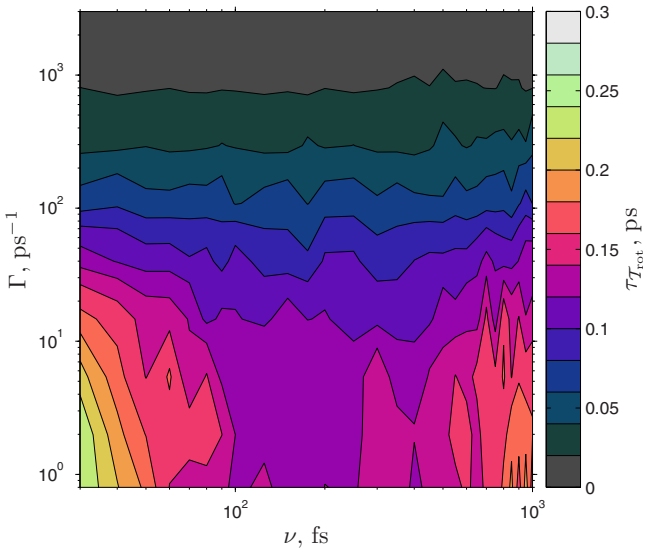

FIG. 10. (Color online) Rotational temperature relaxation time for the gradient-Langevin thermostat (14)-(15) as a function of the thermostat parameters ν and Γ.

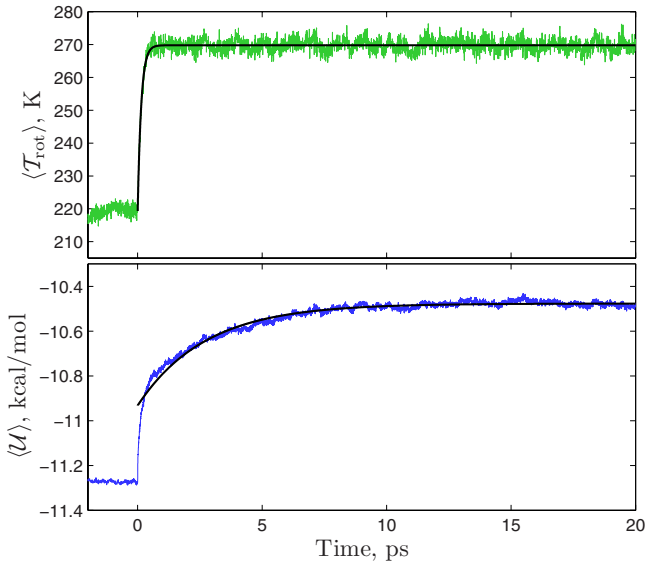

FIG. 12. (Color online) Relaxation dynamics with gradient-Langevin thermostat: $\nu=100$ fs, $\Gamma=0$. Thin lines show relaxation dynamics averaged over seven independent runs, thick lines show the least-squares fit to formula (40).

what surprising finding of this experiment is that even for small values of Γ the relaxation time is much smaller here than in the case of Langevin thermostat (see Fig. 3). As an illustration, we show the relaxation experiment for $\nu=100$ fs and $\Gamma=0$ in Fig. 12. The estimated relaxation time for rotational temperature, $\tau_{\mathcal{T}_{\rm rot}}=0.14$ ps, is much smaller than the corresponding quantity for the Langevin thermostat, even though the relaxation time for the potential energy, $\tau_{\mathcal{U}}=2.7$ ps, is similar. This indicates a very efficient heat transfer between the gradient dynamics of the translational motion and the rotational motion.

The dependence of $\tau_{\mathcal{U}}$ on the thermostat parameters for the gradient-Langevin system shown in Fig. 11 is markedly different than for the Langevin system. In particular, the relaxation time decreases with increasing ν without reaching a minimum value within the range of ν values explored. At the same time, there is little dependence on Γ, except for very large Γ where, similar to the Langevin system, the measurements of the relaxation time are not reliable. Also, note that the relaxation times are much smaller, reaching as low as 0.7 ps for $\nu=1000$ fs, compared to the minimum value of about 2.0 ps for the Langevin system.

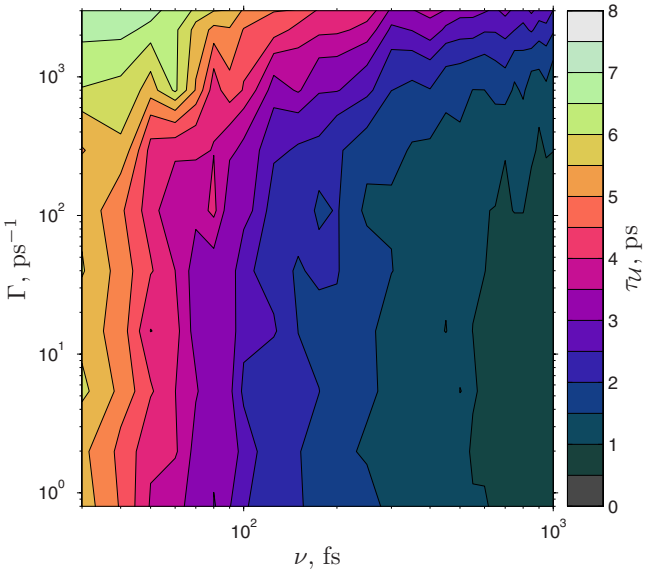

FIG. 11. (Color online) Potential energy relaxation time for the gradient-Langevin thermostat (14)-(15) as a function of the thermostat parameters ν and Γ.

Of course, the direct comparison between the relaxation speeds of gradient-Langevin and Langevin dynamics has to be taken with caution, since, as we mentioned in Sec. II B, the gradient dynamics does not have a natural evolution time. In particular, the mass of the molecule m does not have a specific meaning in the gradient system since it can be rescaled to any value together with h and ν [see Eq. (14)]. Computationally, the relaxation speed depends on the time step h and, while with $\nu=1000$ fs the gradient-Langevin scheme becomes unstable for h larger than 0.2 fs, the Langevin scheme remains stable up to about $h=10$ fs for the optimal values of $\gamma=4.0$ ps^{-1} and $\Gamma=10$ ps^{-1}.

The dependence of discretization error in measured quantities on h for the gradient-Langevin scheme is shown in Fig. 13. As in the case of Langevin A and B, we clearly see the linear dependence of $\langle \mathcal{T}_{\rm rot} \rangle_h$, and $\langle \mathcal{U} \rangle_h$ on h^2. The estimated slopes in Eq. (44) are $C_{\mathcal{T}_{\rm rot}}=-0.38$ K/fs^2 and $C_{\mathcal{U}}=-0.029$ kcal/mol fs^2. Unfortunately, for this value of ν the gradient-Langevin numerical integrator becomes unstable for time steps h exceeding 1 fs, which is rather small, given that Langevin A and B integrator are stable for h up to about 10 fs. Still, given the observed efficient heat transfer from the gradient subsystem for translational dynamics to the rotational dynamics (see Fig. 12 and related discussion), it might be of interest to construct numerical methods for the gradient-Langevin system (14)-(15) with better stability properties than those of system (32)-(23); this has not been considered in this paper.

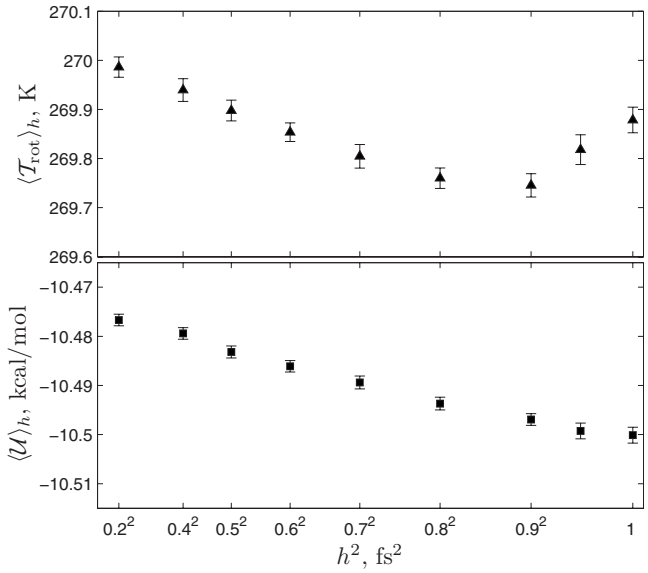

FIG. 13. Dependence of the approximated average properties of a system of 2000 TIP4P water molecules on the integration time step h for the gradient-Langevin numerical method. The system is equilibrated with the thermostat parameters $\nu=200$ fs, $\Gamma=5.0$ ps^{-1}, and $T=270$ K. The quantities $\langle \mathcal{T}_{\rm rot} \rangle_h$, and $\langle \mathcal{U} \rangle_h$ are denoted by circles and squares, respectively. Error bars reflect 95% confidence intervals in the obtained results estimated from block averages.

V. SUMMARY

The new stochastic thermostats presented in this paper are appropriate for quaternion-based rigid body models. They are written in the form of Langevin equations and gradient-Langevin system (gradient subsystem for the translational degrees of freedom and Langevin subsystem for the rotational degrees of freedom). The obtained stochastic systems preserve the unit length of the rotational coordinates in the quaternion representation of the rigid body dynamics. The thermostats allow coupling both translational and rotational degrees of freedom to the heat bath. As it is shown in the numerical tests with the TIP4P rigid model of water, the Langevin thermostat relaxes to an equilibrium faster when not only translational degrees of freedom but also rotational ones are thermostated. It turns out that there is an optimal range of the strength of coupling to the heat bath. In contrast, the gradient-Langevin thermostat has a monotone dependence of relaxation time on the thermostat parameters. In the case of the Langevin thermostat, two quasisymplectic second-order (in the weak sense) integrators are constructed and compared in the numerical tests. For the gradient-Langevin thermostat, a Runge–Kutta second-order method is proposed. All the methods preserve the unit length of the rotational coordinates. The numerical experiments demonstrate the efficiency of the proposed thermostating technique.

Relaxation times for the gradient-Langevin thermostat are smaller than for the Langevin thermostat. However, the numerical methods proposed for the Langevin system have better stability properties than the scheme used for numerical integration of the gradient-Langevin system. In our experimental study, the use of the Langevin thermostat together with the quasisymplectic integrators was computationally significantly more efficient than thermostating via the gradient-Langevin system and the numerical scheme for it.

ACKNOWLEDGMENTS

The work of R.L.D. and R.H. was supported by the EPSRC research under Grant No. GR/T27105/01 which is gratefully acknowledged. One of the authors (R.L.D.) did part of the work during his study leave granted by the University of Leicester. The computations were performed on the University of Leicester Mathematical Modeling Centre's cluster, which was purchased through the HEFCE Science Research Investment Fund.

APPENDIX A: THE STATIONARY FOKKER-PLANCK EQUATION FOR LANGEVIN-TYPE EQUATIONS

The stationary Fokker–Planck equation corresponding to Eqs. (6) and (7) has the form (see, e.g., Refs. 5 and 16)

$$L^*\rho = 0, \tag{A1}$$

where

$$\begin{aligned} L^*\rho := \sum_{j=1}^{n} \Bigg\{ & \sum_{i=1}^{3} \frac{b_{ii}^2(r^j)}{2} \frac{\partial^2 \rho}{(\partial p_i^j)^2} + \sum_{i=1}^{4} \frac{1}{2} \frac{\partial^2}{(\partial \pi_i^j)^2} (B_{ii}^2(q^j,\pi^j)\rho) \\ & + \nabla_{p^j} \cdot [\gamma g(p^j,r^j)\rho] - \nabla_{q^j} \cdot \left(\nabla_{\pi^j} \sum_{l=1}^{3} V_l(q^j,\pi^j)\rho \right) \\ & + \nabla_{\pi^j} \cdot \Bigg[\Bigg(\nabla_{q^j} \sum_{l=1}^{3} V_l(q^j,\pi^j) + \nabla_{q^j} U(\mathbf{r},\mathbf{q}) \\ & + \Gamma G(q^j,\pi^j) \Bigg) \rho \Bigg] \Bigg\} - \frac{1}{m} \nabla_{\mathbf{r}} \cdot (\mathbf{p}\rho) \\ & + \nabla_{\mathbf{p}} \cdot [\nabla_{\mathbf{r}} U(\mathbf{r},\mathbf{q})\rho]. \end{aligned}$$

To find relations between γ, Γ, g, G, b, and B such that system (6)-(7) possesses the Gibbsian stationary measure with the density $\rho(\mathbf{r},\mathbf{p},\mathbf{q},\boldsymbol{\pi})$ from Eq. (5), we substitute ρ in Eq. (A1). After some calculations, we get the required relations,

$$\frac{\beta}{m} \frac{b_{ii}^2}{2} \left[\frac{\beta}{m} (p_i^j)^2 - 1 \right] + \gamma \frac{\partial g_i}{\partial p_i^j} - \gamma \frac{\beta}{m} g_i p_i^j = 0, \tag{A2}$$

and

$$\begin{aligned} \beta \frac{B_{ii}^2}{2} & \left[\beta \left(\frac{\partial H}{\partial \pi_i^j} \right)^2 - \frac{\partial^2 H}{(\partial \pi_i^j)^2} \right] + \left(\frac{\partial B_{ii}}{\partial \pi_i^j} \right)^2 + B_{ii} \frac{\partial^2 B_{ii}}{(\partial \pi_i^j)^2} \\ & - \beta B_{ii} \frac{\partial B_{ii}}{\partial \pi_i^j} \frac{\partial H}{\partial \pi_i^j} + \Gamma \frac{\partial G_i}{\partial \pi_i^j} - \Gamma \beta G_i \frac{\partial H}{\partial \pi_i^j} = 0. \end{aligned} \tag{A3}$$

For constant b_{ii} and B_{ii}, relations (A2) and (A3) take the simpler form (10).

APPENDIX B: EQUATIONS FOR THE BODY-FIXED ANGULAR VELOCITIES

Let us fix a molecule and write the equations for the body-fixed angular velocities ω_x, ω_y, and ω_z corresponding to the rotational Langevin subsystem (13). To this end, we recall[10] that

$$\omega_x = 2(S_1Q)^{\mathsf{T}}\dot{Q}, \quad \omega_y = 2(S_2Q)^{\mathsf{T}}\dot{Q}, \quad \omega_z = 2(S_3Q)^{\mathsf{T}}\dot{Q}.$$

Then we obtain

$$d\omega_x = \left(\frac{\tau_1}{I_1} + \frac{I_2 - I_3}{I_1}\omega_y\omega_z\right)dt - \frac{M\Gamma}{4I_1}\omega_x dt + \frac{1}{I_1}\sqrt{\frac{2M\Gamma}{\beta}}d\Upsilon_1,$$

$$d\omega_y = \left(\frac{\tau_2}{I_2} + \frac{I_3 - I_1}{I_2}\omega_x\omega_z\right)dt - \frac{M\Gamma}{4I_2}\omega_y dt + \frac{1}{I_2}\sqrt{\frac{2M\Gamma}{\beta}}d\Upsilon_2,$$

$$d\omega_z = \left(\frac{\tau_3}{I_3} + \frac{I_1 - I_2}{I_3}\omega_x\omega_y\right)dt - \frac{M\Gamma}{4I_3}\omega_z dt + \frac{1}{I_3}\sqrt{\frac{2M\Gamma}{\beta}}d\Upsilon_3, \tag{B1}$$

where τ_i are the torques, $\tau_i = -\frac{1}{2}(S_iQ)^{\mathsf{T}}\nabla_q U$, and $d\Upsilon_i = \frac{1}{2}\Sigma_{j=1}^{4}(S_iQ)_j dW_j$, which can be interpreted as random torques. For $\Gamma = 0$, Eq. (B1) coincides with the equations for the angular velocities in Ref. 10. We also note that due to the form of Hamiltonian (1) the auxiliary velocity ω_0 used in Ref. 10 in the derivation of the Hamiltonian system for rigid body dynamics is identically equal to zero.

[1] P. H. Hünenberger, Adv. Polym. Sci. **173**, 105 (2005).
[2] B. Leimkuhler and S. Reich, *Simulating Hamiltonian Dynamics* (Cambridge University Press, Cambridge, 2005).
[3] R. Skeel, in *Graduate Student's Guide to Numerical Analysis '98*, edited by M. Ainsworth, J. Levesley, and M. Marletta (Springer, New York, 1999), pp. 118–176.
[4] J. A. Izaguirre, D. P. Catarello, J. M. Wozniak, and R. D. Skeel, J. Chem. Phys. **114**, 2090 (2001).
[5] C. Soize, *The Fokker-Planck Equation for Stochastic Dynamical Systems and its Explicit Steady State Solutions* (World Scientific, Singapore, 1994).
[6] J. C. Mattingly, A. M. Stuart, and D. J. Higham, Stochastic Proc. Appl. **101**, 185 (2002).
[7] G. N. Milstein and M. V. Tretyakov, Physica D **229**, 81 (2007).
[8] E. Vanden-Eijnden and G. Ciccotti, Chem. Phys. Lett. **429**, 310 (2006).
[9] X. Sun, T. Lin, and J. D. Gezelter, J. Chem. Phys. **128**, 234107 (2008).
[10] T. F. Miller III, M. Eleftheriou, P. Pattnaik, A. Ndirango, D. Newns, and G. J. Matyna, J. Chem. Phys. **116**, 8649 (2002).
[11] W. L. Jorgensen, J. Chandrasekhar, J. Madura, R. W. Impey, and M. L. Klein, J. Chem. Phys. **79**, 926 (1983).
[12] D. J. Evans, Mol. Phys. **34**, 317 (1977); D. J. Evans and S. Murad, *ibid.* **34**, 327 (1977).
[13] S. L. Altmann, *Rotations, Quaternions, and Double Groups* (Dover, New York, 1986).
[14] W. B. Heard, *Rigid Body Mechanics* (Wiley, New York, 2006).
[15] Following the standard notation of the SDE theory, we use capital letters to denote the SDE solution and small letters for the initial data and for corresponding "dummy" variables.
[16] R. Z. Hasminskii, *Stochastic Stability of Differential Equations* (Sijthoff & Noordhoff, Alphen aan den Rijn, 1980).
[17] D. Talay, Markov Processes Relat. Fields **8**, 163 (2002).
[18] E. Nelson, *Dynamical Theories of Brownian Motion* (Princeton University Press, Princeton, 1967).
[19] G. N. Milstein and M. V. Tretyakov, I.MA J. Numer. Anal. **23**, 593 (2003).
[20] G. N. Milstein and M. V. Tretyakov, *Stochastic Numerics for Mathematical Physics* (Springer, New York, 2004).
[21] G. N. Milstein, Yu. M. Repin, and M. V. Tretyakov, SIAM (Soc. Ind. Appl. Math.) J. Numer. Anal. **39**, 2066 (2002).
[22] G. Bussi and M. Parrinello, Phys. Rev. E **75**, 056707 (2007).
[23] D. Talay, Stoch. Stoch. Rep. **29**, 13 (1990).
[24] R. Handel, R. L. Davidchack, J. Anwar, and A. Brukhno, Phys. Rev. Lett. **100**, 036104 (2008).
[25] D. Talay and L. Tubaro, Stoch. Anal. Appl. **8**, 483 (1990).